Journal of Pharmaceutical and Biomedical Analysis 49 (2009) 1226–1232

Contents lists available at ScienceDirect

Journal of Pharmaceutical and Biomedical Analysis

journal homepage: www.elsevier.com/locate/jpba

# Determination of osthol and its metabolites in a phase I reaction system and the Caco-2 cell model by HPLC-UV and LC–MS/MS

Zhenting Yuan[a,b], Haiyan Xu[b], Ke Wang[a], Zhonghua Zhao[a], Ming Hu[b,*]

[a] No. 230 Hospital in Dandong, Dandong 118000, PR China
[b] Department of Pharmacological and Pharmaceutical Sciences, College of Pharmacy, University of Houston, Houston, TX77030, USA

ARTICLE INFO

*Article history:*
Received 31 July 2008
Received in revised form 1 December 2008
Accepted 1 December 2008
Available online 9 December 2008

*Keywords:*
Osthol
Caco-2 cell model
Microsomes
Phase I
HPLC
LC-MS/MS

ABSTRACT

A straightforward and sensitive reversed-phase high-performance liquid chromatography (HPLC) assay was developed and validated for the analysis of osthol and its phase I metabolites (internal standard: umbelliferone). The method was validated for the determination of osthol with respect to selectivity, precision, linearity, limit of detection, recovery, and stability. The linear response range was 0.47–60 μM, and the average recoveries ranged from 98 to 101%. The inter-day and intra-day relative standard deviations were both less than 5%. Using this method, we showed that more than 80% of osthol was metabolized in 20 min in a phase I metabolic reaction system. Transport experiments in the Caco-2 cell culture model indicated that osthol was easily absorbed with high absorptive permeability ($>10 \times 10^{-6}$ cm/s). The permeability did not display concentration-dependence or vectorial-dependence and is mildly temperature sensitive (activation energy less than 10 kcal/mol), indicating passive mechanism of transport. When analyzed by LC–MS/MS, five metabolites were detected in a phase I reaction system and in the receiver side of a modified Caco-2 cell model, which was supplemented with the phase I reaction system. The major metabolites appeared to be desmethyl-osthol and multiple isomers of dehydro-osthol. In conclusion, a likely cause of poor osthol bioavailability is rapid phase I metabolism via the cytochrome P450 pathways.



## 1. Introduction

Osthol (Fig. 1) is a major bioactive ingredient isolated from a Chinese medicinal herb *Cnidium monnieri* (L.) *cusson* [1,2], which has been used for treatment of impotence, pain in female genitalia, and suppurative dermatitis (as an antipruritogenic agent) in the traditional Chinese medicine. Reports of pharmacological activities of osthol in modern literatures ranged from anticancer [3–5], anti-allergic action [6], androgenic effects [7], prevention of hepatitis [8] and antibacterial to anticoagulant [9]. The clinical utility of this phytochemical is limited due to its low bioavailability in vivo [10–13]. Even though there have been reports of its pharmacokinetic behaviors in vivo in rats [10,11] and rabbits [12,13], there are no reports concerning its mechanisms of absorption and metabolism. Here, we established a simple, rapid, accurate and specific liquid chromatography method to measure osthol and used it to determine the absorption mechanisms of osthol in Caco-2 cell model and its metabolism in a phase I (cytochrome P450) reaction system.

We have chosen the Caco-2 model system for the current study because it is a commonly used model system to classify a drug's absorption characteristics. The model was used by FDA in its Biopharmaceutical Classification System (http://www.fda.gov/cder/OPS/BCS_guidance.htm) designation. Permeabilities obtained from this model may be used to determine whether absorption of a compound is good (>75%), or poor (<10%).

## 2. Experimental

### 2.1. Chemicals and reagents

Osthol (OS) was isolated from *C. monnieri*. The purity of osthol was determined by HPLC (>99.6%) using the authentic osthol standard purchased from the National Institute for the Control of Pharmaceutical and Biological Products (Beijing, China). Nicotinamide adenine dinucleotide phosphate (NADP), glucose-6-phosphate sodium (6-DP), glucose-6-phosphate dehydrogenase (6-DPD), magnesium chloride ($MgCl_2$), phosphoric acid ($H_3PO_4$), HBSS (Hank's balanced salt solution) powder, sodium citrate, potassium phosphate dibasic ($K_2HPO_4$), PEG600 and umbelliferone were purchased from Sigma Chemical Co. (St. Louis, USA).

* Corresponding author. Tel.: +1 713 795 8320; fax: +1 713 795 8305.
*E-mail address:* mhu@uh.edu (M. Hu).

0731-7085/$ – see front matter © 2008 Elsevier B.V. All rights reserved.
doi:10.1016/j.jpba.2008.12.001

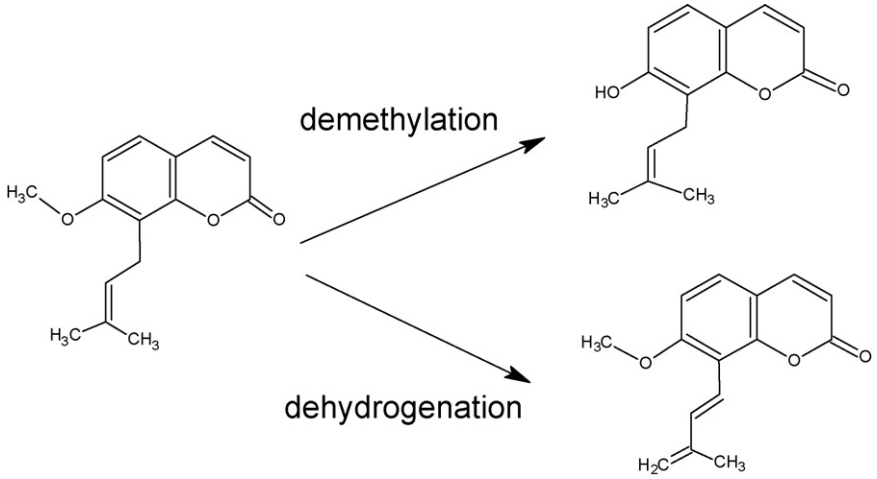


**Fig. 1.** Chemical structures of osthol and its phase I metabolites.

### 2.2. Chromatographic conditions

#### 2.2.1. HPLC conditions

The HPLC is consisted of HP 1090 ChemStation with a diode array detector. Chromatographic separation was carried out on a reversed-phase $C_{18}$ column (4.6 mm × 250 mm, 5 μm, Diamonsil). Absorbance was monitored at 320 nm. The program of gradient elution used is as follows: 0–20 min, 45–75% mobile phase A; 20–22 min, 75% mobile phase A; 22–23 min, 75–45% mobile phase A. The mobile phase A consisted of 100% acetonitrile (ACN) whereas the mobile phase B was an aqueous solution containing 0.6% triethylamine and 0.45% formic acid (pH 2.85).

#### 2.2.2. UPLC–MS/MS conditions

An API 3200 Qtrap triple quadrupole mass spectrometer (Applied Biosystem/MDS SCIEX, Foster City, CA, USA) equipped with an atmospheric pressure chemical ionization (APCI) source was operated in positive ion mode to perform the analysis. The main working parameters for the mass spectrometer were set as following: ion source temperature, 300 °C; the nebulizer current, 1.0 μA; the nebulizer gas (zero air, GAS1), 40 psi; curtain gas (nitrogen gas), 20 psi. Osthol and its phase I metabolites were identified by MS full scan and $MS^2$ full scan modes.

UPLC conditions for analyzing osthol and its metabolites were: system, Waters AcQuity™ with DAD detector; column, Acquity UPLC BEH $C_{18}$ column (50 mm × 2.1 mm I.D., 1.7 μm, Waters, Milford, MA, USA); mobile phase A, water; mobile phase B, 100% acetonitrile; gradient, 0–10.0 min, 0–60% B, 10.0–10.5 min, 60–0% B, 10.5–10.8 min, 0% B; wavelength, 254 nm; flow rate, 0.5 ml/min; and injection volume, 10 μl.

### 2.3. Metabolism and determination of osthol in phase I reaction system

#### 2.3.1. Rat liver microsomes (RLM) preparation

RLM were prepared from male adult Sprague–Dawley rats (200–250 g) using a procedure adopted from the literature with minor modification [14]. Briefly, eight fresh rat livers were harvested from euthanized rats. The livers were perfused and washed with ice-cold saline, weighed and minced. Minced livers were homogenized using a motorized homogenizer (4 strokes) in ice-cold homogenization buffer (50 mM potassium phosphate, 250 mM sucrose, 1 mM EDTA, pH 7.4) and centrifuged at 7700 × *g* for 15 min at 4 °C. The supernatant collected was then centrifuged again at 18,500 × *g* for 15 min at 4 °C. After the pellet was discarded, the supernatant was centrifuged again at 100,000 × *g* for 1 h at 4 °C to yield microsomal pellets. The microsomes were resuspended in washing buffer (10 mM potassium phosphate, 0.1 mM EDTA, 150 mM KCl, pH 7.4), and re-pelleted at 100,000 × *g* for 1 h at 4 °C to yield microsomes. The microsomes were then resuspended in 250 mM sucrose, aliquoted into vials (0.5 ml per vial) and stored at −80 °C until use. The concentration of microsomal protein was determined by the Bio-Rad protein assay (Bio-Rad laboratories, Hercules, CA, USA) using bovine serum albumin as the standard.

#### 2.3.2. Phase I reaction system

The incubation procedures for phase I reaction using liver microsomes were as follows: (1) mix microsomes (final concentration ≈0.5 mg protein/ml), NADP (2.61 mM), 6-DP (6.6 mM), $MgCl_2$ (6.6 mM), different concentrations of substrates in a 50 mM potassium phosphate buffer (pH 7.4), and 6-DPD in 5 mM sodium citrate solution (40 U/ml, add last); (2) incubate the mixture (final volume = 200 μl) at 37 °C for a pre-determined period of time (e.g., 1 h); and (3) end the reaction with the addition of 400 μl of umbelliferone (as the internal standard, IS) solution in methanol. The samples were vortexed for 0.5 min, centrifuged at 15,000 rpm/min for 15 min, and 240 μl of supernatant was injected into HPLC system for analysis (See Section 2.2.1).

#### 2.3.3. Preparation of standard and quality control samples

Stock solutions of osthol was prepared and diluted to 500 μM with acetonitrile. Stock solution of IS was prepared and diluted to 3 μg/ml (or 18.53 μM) with acetonitrile. Calibration curves were prepared by spiking 1.7 μl of the appropriate standard solution to 200 μl of inactivated phase I reaction system (boiled for 2 min at 100 °C) with the effective concentrations of 60, 30, 15, 7.5, 3.75, 1.88, 0.94 and 0.47 μM. Quantification was based on the peak area ratios of osthol to that of the internal standard and standard curves in the form of $y = A + Bx$, where $y$ represents the concentration of analyte and $x$ represents the ratios of analyte peak area to that of internal standard. The linear equation was derived using weighted ($1/x^2$) least squares linear regression. To evaluate linearity, calibration curves were prepared and analyzed in duplicate on 3 separate days. The accuracy and precision were also determined by assay ($n = 6$) to QC samples at three concentration levels on 3 different validation days. The accuracy was expressed by (mean observed concentration)/(spiked concentration) × 100% and the precision by relative standard deviation (RSD%). The concentration of each sample

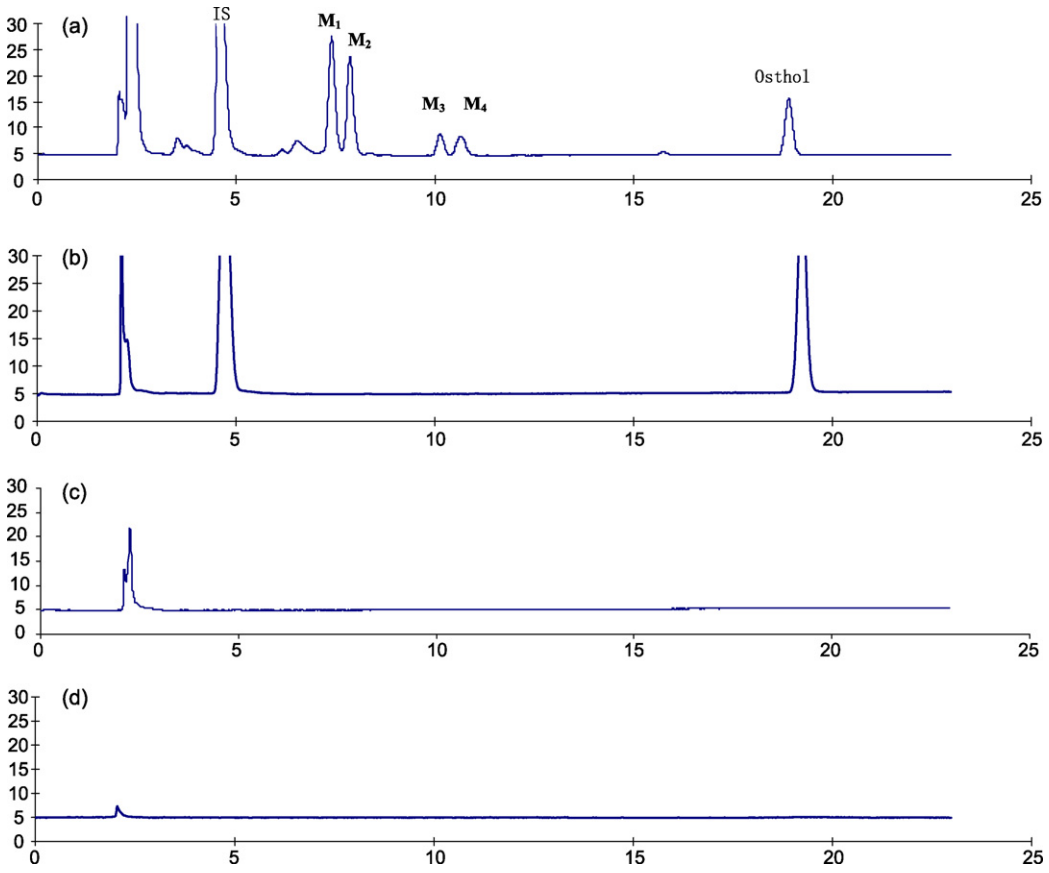


**Fig. 2.** Representative HPLC chromatograms of osthol and IS in phase I reaction system (a), OS and IS in inactivated phase I reaction system and Caco-2 cell model (b), blank phase I reaction system (c), and blank HBSS (d).

was determined using the calibration curve and analyzed on the same day. The short-term stability was examined by keeping replication of the osthol solution in inactivated phase I reaction system and HBSS at 4 °C and 37 °C for 72 h.

### 2.4. Transportation and metabolism of osthol in Caco-2 cell model

#### 2.4.1. Preparation of calibration standards

Standard solution was prepared using the same procedure described above except that the 200 μl HBSS was used to replace the 200 μl the inactivated phase I reaction system.

#### 2.4.2. Cell culture

Cell culture conditions for growing Caco-2 cells have been described previously [15]. The seeding density was 100,000 cells/cm$^2$ (4.2 cm$^2$ per monolayer), and Dulbecco's modified Eagle's medium supplemented with 10% fetal bovine serum was used as the growth medium. Quality control criteria were the same as described previously [16]. Cell monolayer from 19 to 22 days past seeding was used for the experiments.

#### 2.4.3. Transport experiments of various concentrations of osthol in the Caco-2 cell model

The protocols for performing transport experiments were similar to those described previously [17]. In brief, the cell monolayer was washed three times with 37 °C 2.5 ml HBSS (pH 7.4). The transepithelial electrical resistance values were measured, and those with the values less than 420 Ω/cm$^2$ were discarded. Various concentrations (ranging from 5, 10, 15 μM) of osthol were loaded on either the apical (AP) or basolateral (BL) side of the Caco-2 cell monolayer, and the concentration of osthol and its metabolites at both sides were measured by HPLC-UV. Six samples (0.4 ml) were taken at different times from both donor and receiver side (total volume of each chamber was 2.5 ml), and the same volume of solution was replaced with original donor or receiver solution after each sampling. To each sample a 0.4 ml of IS solution was added and the mixtures were then vortexed for 0.5 min and centrifuged at 15,000 rpm/min for 15 min. A 240 μl portion of each supernatant was injected into the HPLC system for quantitation. Standards were processed similarly.

#### 2.4.4. Transport experiments of osthol with the phase I reaction system on the BL side in Caco-2 cell model

For the transport experiments of osthol with the phase I reaction system, 10 μM osthol in HBSS was loaded on the AP side and the phase I reaction system was loaded on the BL side in the Caco-2 cell monolayer. The other experimental procedures are the same as those described previously.

#### 2.4.5. Effect of temperature on transport of osthol across Caco-2 cell monolayer

For the transport experiments of osthol in the Caco-2 cell model at 4 °C, 25 °C and 37 °C, 10 μM osthol in HBSS was loaded on the AP side and HBSS was loaded on the BL side in the Caco-2 cell monolayer. The other experimental procedures are the same as those described previously.

### 2.5. Identify of metabolites of osthol in phase I reaction system and Caco-2 cell model

After metabolic reaction samples were obtained following phase I reaction, 1 ml of the sample and 0.2 ml of ACN were mixed

**Table 1**
Recovery and precision for the analysis of osthol in sample matrix.

| Added C (μM) | Found C (μM) | Inter-day RSD (%) | Intra-day RSD (%) |
|---|---|---|---|
| In phase I reaction system | | | |
| 1.50 | 1.49 | 2.89 | 3.61 |
| 30.0 | 30.07 | 3.37 | 3.92 |
| 60.0 | 59.67 | 4.16 | 4.87 |
| In Caco-2 transport media | | | |
| 1.50 | 1.48 | 3.50 | 4.61 |
| 30.0 | 29.96 | 4.09 | 3.97 |
| 60.0 | 59.67 | 3.19 | 4.73 |

and vortexed to precipitate microsomal protein by centrifugation at 15,000 rpm/min for 15 min. The supernatant was dried under vacuum. The residue was reconstituted with 0.2 ml of 10% ACN in water. The solution was vortexed for 1 min and centrifuged at 15,000 rpm/min for 15 min, and 10 μl of the supernatant was injected for LC/MS/MS analysis.

## 3. Results and discussion

### 3.1. Selectivity

Selectivity was assessed by comparing the chromatograms of 6 different batches of blank matrix from phase I reaction system with the corresponding spiked matrix. Fig. 2 shows the typical chromatograms of a blank, a spiked matrix sample with osthol and I.S., and a sample from phase I reaction or Caco-2 model. There was no significant interference substances observed at the retention times of the analyses. Typical retention times for I.S., $M_1$, $M_2$, $M_3$, $M_4$ and osthol were 4.7, 7, 7.9, 10.2, 10.7 and 18.9 min, respectively. Meanwhile, the specificity was verified by comparing retention times of osthol and its metabolites and internal standard. The differences were less than 1%.

### 3.2. Linearity of calibration curves and lower limits of quantification (LLOQ)

Correlation coefficients (>0.999) of plotted duplicate calibration curves indicated that the calibration curves were linear over the concentration range of 0.47–60 μM for osthol. Typical standard curve was $y = 0.0224x + 7.0 \times 10^{-5}$ ($r = 0.9998$) for experiment of phase I reaction system and $y = 0.0332x - 0.0069$ ($r = 0.9992$) for Caco-2 cell model, respectively, where $y$ represents the ratios of peak area of analytes to that of internal standard, and $x$ represents the concentrations of analytes. The lower limit of quantification (LLOQ) was defined as the lowest concentration on the calibration curve for which an acceptable accuracy of ±15% and a precision below 15% were obtained. The present method offered LLOQ of 0.47 μM and the lower limit of detection (LLOD) of 0.2 μM for osthol. These LLOQ and LLOQ values were similar to those reported by Zhou et al. [18] and the LLOQ level was also similar to the one reported by Li et al. [11].

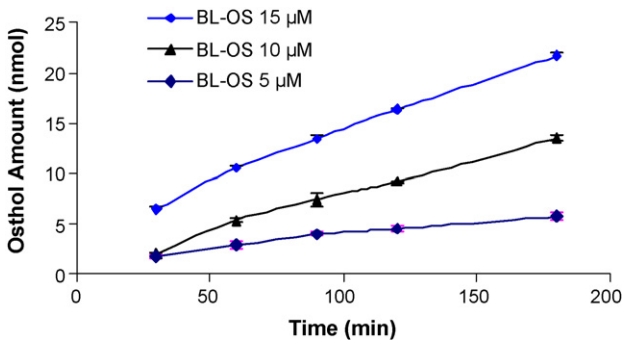


**Fig. 3.** Effects of different concentrations on transport of osthol across Caco-2 cell monolayer. Each data point is the average of three determinations and the error bar is the standard deviation of the mean.

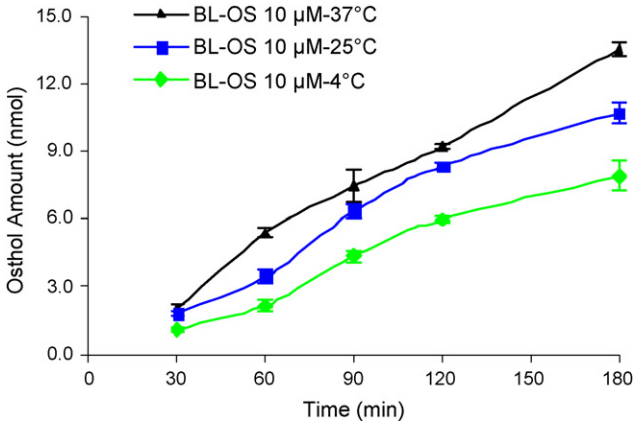


**Fig. 4.** Transport of osthol across Caco-2 cell monolayers at different temperatures. Each data point is the average of three determinations and the error bar is the standard deviation of the mean.

### 3.3. Recovery and precision

The intra- and inter-day precision and accuracy for osthol were evaluated by assaying the samples with low, medium and high concentration. The precision was calculated. In this assay, as shown in Table 1, for each level of osthol, the intra-day precision was 4.87% or less, and the inter-day precision was 4.16% or less. These results demonstrated that the recovery and precision values were

**Table 2**
Apparent permeabilities of osthol across Caco-2 cell monolayer ($n = 3$) at different concentrations.

| Concentration (μM) | $P_{AP} \times 10^{-6} \pm$ SD cm s$^{-1}$ | $P_{BL} \times 10^{-6} \pm$ SD cm s$^{-1}$ | Ratio $P_{BL}/P_{AP}$ |
|---|---|---|---|
| 5.00 | 24.3 ± 0.73 | 24.4 ± 1.4 | 1.00 |
| 10.00 | 31.2 ± 0.3 | 29.4 ± 2.5 | 0.94 |
| 15.00 | 28.5 ± 0.50 | 29.5 ± 1.3 | 1.04 |

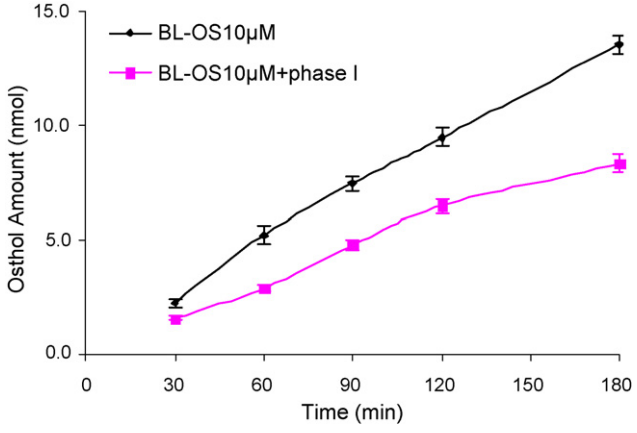


**Fig. 5.** Effects of presence of a phase I reaction system on the BL side on the transport of osthol across the Caco-2 cell monolayers. Each data point is the average of three determinations and the error bar is the standard deviation of the mean.

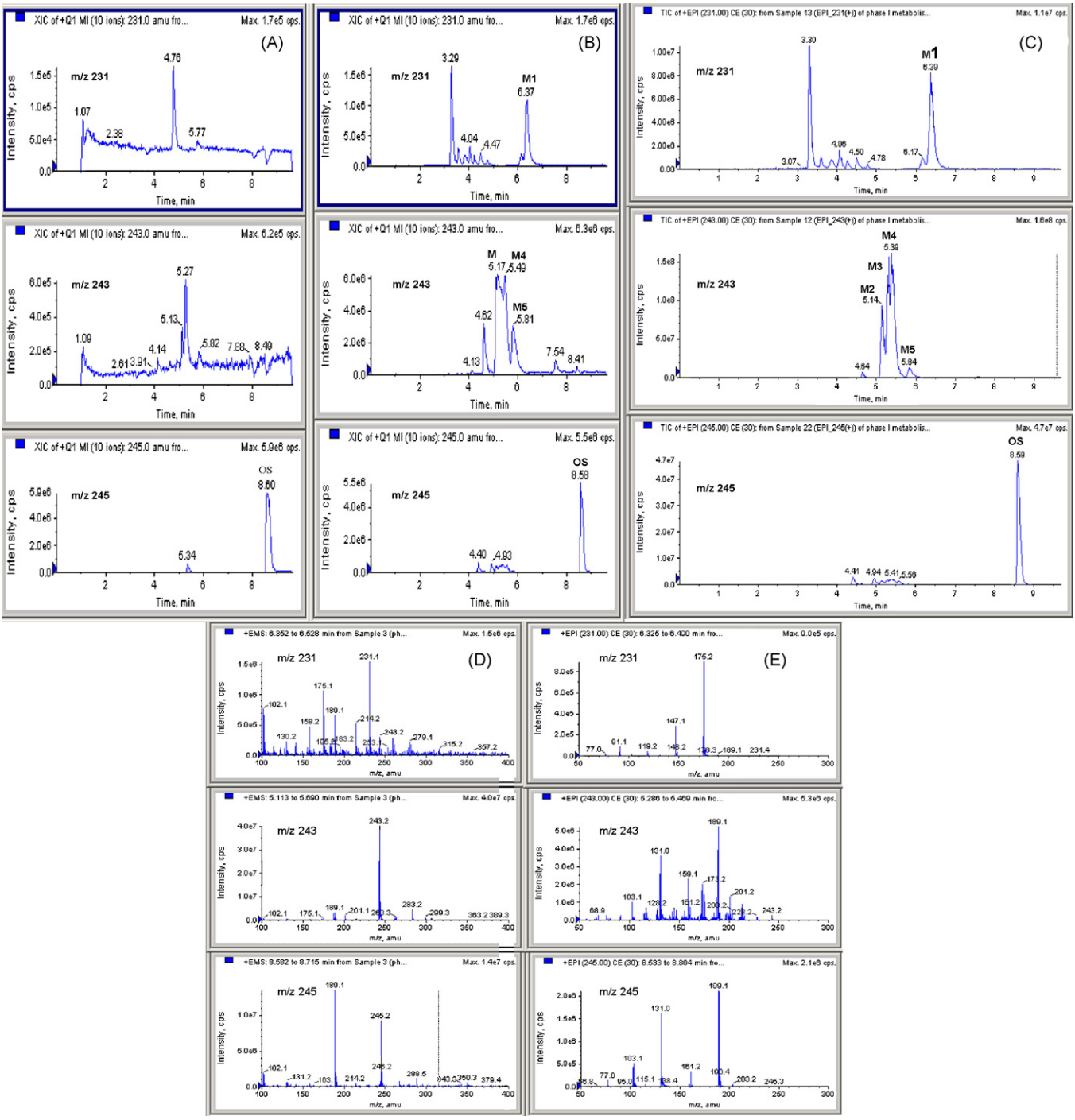


**Fig. 6.** Representative LC–MS chromatograms and MS spectra of osthol and its metabolites. The conditions for generating these diagrams were stated in the Section 2. (A) Selective ion monitoring chromatogram of a control sample; (B) Selective ion monitoring chromatogram of a liver microsome sample; (C) $MS^2$ full scan chromatogram of a liver microsome sample; (D) First stage full scan spectra of osthol and its metabolites; (E) $MS^2$ full scan spectra of osthol and its metabolites.

within the acceptable range and the method was accurate and precise. There are again similar to the methods reported previously [11,18].

### 3.4. Stability

The stability of the osthol solution in heat-inactivated phase I reaction system and HBSS at 4 and 37 °C was checked for 72 h. The results showed that osthol was stable over the experimental period of 72 h.

### 3.5. Metabolism and determination of osthol in phase I reaction system

Time dependent metabolisms of osthol in phase I reaction system was studied. The results showed rapid metabolism of osthol. 40% of osthol was lost in the first 5 min, and another 40% was lost in the next 15 min, resulting in 80% loss within 20 min (not shown). Four main metabolites ($M_1$, $M_2$, $M_3$, $M_4$) were detected following phase I reaction based on analysis with HPLC-UV (Fig. 2). A UPLC/MS/MS method was used to further identify several of the unknown metabolites (later).

### 3.6. Effect of concentrations of osthol on transport of osthol across Caco-2 cell monolayer

Transport of 5, 10, 15 μM solution of osthol was studied in the Caco-2 cell model. The results indicated that amount transported increased with loading concentration, but permeability was essentially the same (Fig. 3 and Table 2). Since osthol has high absorptive permeability (>$20 \times 10^{-6}$ cm/s) across the Caco-2 cell model, it is expected to be rapidly and completely absorbed, based on a Biopharmaceutical Classification System proposed by US FDA. Further, there were no significantly differences in the ratios of $P_{BL}$ to $P_{AP}$ at three concentrations, suggesting that the absorption is via passive diffusion. This permeability across Caco-2 cell monolayers was significantly higher than the one reported by Yang et al. [19], who also showed similar apical to basolateral and basolateral to apical transport of osthol.

### 3.7. Effect of temperature on transport of osthol across Caco-2 cell monolayer

Transport of osthol (10 μM) was studied in the Caco-2 cell model at three different temperatures to determine if the transport is active. The results indicated that amount transported increased with rising temperature (Fig. 4), but activation energy is quite moderate at 4.14 kcal/mol (Arrhenius plot not shown), which is consistent with a passive diffusion mechanism for its absorption. Earlier, it was shown that the vectorial transport of this compound was not affected by a MRP transporter inhibitor MK571 [19], but the weak temperature dependence shown here provides a critical evidence to show that a transporter is not involved in the active transepithelial transport of osthol.

### 3.8. Transport of osthol in Caco-2 cell model with the phase I reaction system on the BL side

Because high permeability of osthol was inconsistent with its poor bioavailability, whereas rapid phase I metabolism was, we decided to determine how absorption of osthol may change when a phase I reaction system was present at the basolateral side to simulate the dynamic effects of phase I metabolism on osthol bioavailability. This is similar to a previous approach of using a hybrid model of Caco-2 cells and human hepatocytes to simulate a model of absorption and metabolism [20,21]. We determined the transport of osthol in Caco-2 cell model with or without the phase I reaction system on the BL side in an effort to simulate this dynamic effect. As can be seen in Fig. 5, the amount ($8.33 \pm 0.37$ nmol vs. $13.51 \pm 0.32$ nmol) and the rate of osthol transport in the presence of a phase I reaction system is significantly lower than that those without the phase I reaction system. The result illustrates that osthol is rapidly metabolized by phase I reaction system after crossing the Caco-2 cell monolayer and several metabolites were detected (see below).

### 3.9. Identification of osthol and its metabolites by LC-MS/MS

Compare to the control samples using inactivated microsomes, a total of four new major peaks were found in the microsome samples (Fig. 6A and B) using the total ion current (TIC) MS spectrum. The retention time of osthol was 8.6 min and peaks at 5.2, 5.5, 5.8, and 6.4 min were referred as metabolite $M_2$, $M_3/M_4$, $M_5$ and $M_1$, respectively (Fig. 6B). The single-stage full scan mass spectra showed that the pseudomolecular ions $[M+H]^+$ of parent drug, $M_1$, $M_2$, $M_3/M_4$ and $M_5$ were at *m/z* 245, *m/z* 231, *m/z* 243, *m/z* 243 and *m/z* 243, respectively (Fig. 6D). The pseudomolecular ion of $M_1$ was 14 Da lower (characteristic of heteratom demethyl metabolite) than that of osthol (Fig. 6D). The $MS^2$ spectrum of $M_1$ showed fragment ions at *m/z* 175 and *m/z* 147. These two daughter ions were 14 Da lower than the diagnostic ions at *m/z* 189 and *m/z* 161 in the $MS^2$ spectrum of osthol, respectively (Fig. 6E), which indicated that $M_1$ had the same pathway of fragmentation as that of osthol (not shown). Based on the above results, $M_1$ was identified as the *O*-desmethyl metabolite of osthol.

Metabolites $M_2$, $M_3/M_4$ and $M_5$ gave the same pseudomolecular ion $[M+H]^+$ at *m/z* 243, which was 2 Da lower (characteristic of lost of a molecule hydrogen) than that of osthol (Fig. 6D). Since it was hard to separate $M_2$, $M_3/M_4$ and $M_5$ and the selectivity and resolution of selective ion scan (SIM) mode are lower than those of $MS^2$ scan mode, $MS^2$ scan mode was used to confirm the identification of metabolites. In the $MS^2$ scan mode, $M_3$ was separated from $M_4$, perhaps due to better resolution of this mode than the TIC mode. Since $M_2$, $M_3$, $M_4$ and $M_5$ had the similar $MS^2$ spectra in that all of their $MS^2$ spectra generated diagnostic ions at *m/z*189, *m/z*161, *m/z*131 and *m/z* 103, which is the same as those generated by the $MS^2$ spectrum of osthol (Fig. 6E), these results suggested that $M_2$, $M_3$, $M_4$ and $M_5$ were the (*cis–trans*) isoforms of dehydro metabolites of osthol.

## 4. Conclusion

A straightforward reversed-phase HPLC-UV method has been developed for the determination of osthol and its metabolites. Selectivity, precision, recovery, sensitivity and linearity of method for analyzing osthol have been validated. The method has been successfully applied to determination of the osthol in transport studies in Caco-2 model and in metabolism studies in a phase I (cytochrome P450) reaction system. The Caco-2 studies indicate that osthol has a high absorptive permeability (>$20 \times 10^{-6}$ cm/s), and its absorption is via passive diffusion. Metabolism studies using a phase I reaction system or using Caco-2 cell model modified with a phase I reaction system in the receiver side indicates that osthol is rapidly metabolized by phase I enzymes to desmethyl-osthol (M1) and four *cis–trans* isomers of dehydro-osthol (M2–M5). Taken together, the application of a newly developed method of osthol analysis show that poor bioavailability of osthol was not the result of poor permeation. On the other hand, rapid metabolism appears to be a major contributor to its poor bioavailability.

## Acknowledgements

The work was supported by NIH GM070737 to M.H. at University of Houston. Z.Y. is also supported by a training grant from No. 230 Hospital, Dandong, Liaoning, China.

## References

[1] X.Y. Zhang, R.D. Xiang, Chin. Trad. Herb. Drugs 28 (1997) 588–590.
[2] Raw and Processed Chinese Herbs, Pharmacopeia of The People's Republic of China, vol. I (J), Pharmacopeia Commission of The People's Republic of China, Chemical Industry Press, Beijing, 2005, pp. 219–220.
[3] T. Fujioka, K. Furumi, H. Fujii, H. Okabe, K. Mihashi, Y. Nakano, H. Matsunaga, M. Katano, M. Mori, Chem. Pharm. Bull. 47 (1999) 96–100.
[4] J. Zhou, W.X. Cheng, Y.H. Xu, D.H. Zhang, D.M. Wang, Teratog. Carcinog. Mutagen. 14 (2002) 231–233.
[5] C. Riviere, L. Goossens, N. Pommery, Nat. Prod. Res. 20 (2006) 909–916.
[6] Z.W. Zhou, X. Shen, X.X. Wu, P.X. Liu, W.Q. Xu, R. Li, Teratog. Carcinog. Mutagen. 19 (2007) 119–121.
[7] S.Y. Chou, C.S. Hsu, K.T. Wang, M.C. Wang, C.C. Wang, Phytother. Res. 21 (2007) 226–230.
[8] T. Okamoto, T. Kobayashi, S. Yoshida, Med. Chem. 3 (2007) 35–44.
[9] S. Rosselli, A. Maggio, G. Bellone, C. Formisano, A. Basile, C. Cicala, A. Alfieri, N. Mascolo, M. Bruno, Planta Med. 73 (2007) 116–120.
[10] T.H. Sai, T.R. Tsai, C.C. Chen, C.F. Chen, J. Pharm. Biomed. Anal. 14 (1996) 749–753.
[11] Y. Li, F. Meng, Z. Xiong, H. Liu, F. Li, J. Chromatogr. Sci. 43 (2005) 426–429.
[12] F. An, S.H. Wang, D.S. Zhang, L. Zhang, J.X. Mu, Acta Pharm. Sin. 38 (2003) 571–573.
[13] Y.R. Gao, L. Zhang, D.S. Zhang, Chin. J. Hosp. Pharm. 25 (2005) 1143–1146.

[14] M. Hu, K. Krausz, J. Chen, X. Ge, J. Li, H.L. Gelboin, F.J. Gonzalez, Drug Metab. Dispos. 31 (2003) 924–931.
[15] Y. Liu, M. Hu, Drug Metab. Dispos. 30 (2002) 370–377.
[16] M. Hu, J. Chen, D. Tran, Y. Zhu, G. Leonardo, J. Drug Target 2 (1994) 79–89.
[17] M. Hu, J. Chen, Y. Zhu, A.H. Dantzig, R.E. Stratford Jr., M.T. Kuhfeld, Pharm. Res. 11 (1994) 1405–1413.
[18] J. Zhou, S.W. Wang, X.L. Sun, Anal. Chim. Acta 608 (2008) 158–164.
[19] X.W. Yang, Q.M. Guo, Y. Wang, Zhong Xi Yi Jie He Xue Bao 6 (2008) 392–398.
[20] C. Li, T. Liu, X. Cui, A.S. Uss, K.C. Cheng, J. Biomol. Screen 12 (2007) 1084–1091.
[21] K.C. Cheng, C. Li, Y. Hsieh, D. Montgomery, T. Liu, R.E. White, J. Pharmacol. Toxicol. Methods 53 (2006) 215–218.